Diamond & Related Materials 19 (2010) 462–465

Contents lists available at ScienceDirect

Diamond & Related Materials

journal homepage: www.elsevier.com/locate/diamond

The effect of surface treatment on oxidation of oxalic acid at nanocrystalline diamond films

A.F. Azevedo *, N.A. Braga, F.A. Souza, J.T. Matsushima, M.R. Baldan, N.G. Ferreira

Instituto Nacional de Pesquisas Espaciais, Av. Astronautas 1758, SJ Campos, SP/12245-970, Brazil

ARTICLE INFO

Available online 13 January 2010

Keywords:
Nanocrystalline
Diamond films
p-Type doped
Wettability
Organic oxidation

ABSTRACT

The surface investigation of undoped and boron doped nanocrystalline diamond (NCD/BDND) films associated to their electrochemical behavior of oxalic acid after four pre-treatments was studied. The films were produced using Hot Filament CVD technique on Si substrate with a gas mixture of $CH_4/H_2/Ar$. Surface pre-treatments were carried out to analyze the surface chemical changes induced by hydrogen and oxygen plasma and as well as cathodic and anodic treatments performed in 0.1 mol L^{-1} $HClO_4$. The films wetting analyzed by contact angle presented a strong dependence of their surface before and after each treatment was also confirmed by the electrochemical response from cyclic voltammograms. Independent of the surface pre-treatments, all the electrodes exhibited response for oxalic acid oxidation, but the electrode submitted to hydrogen plasma presented the lowest starting oxidation potential and the highest current density. Nonetheless, the BDND electrode presented higher oxidation current than that for NCD electrodes, after all pre-treatments studied. The use of square wave voltammetry with BDND electrode treated by hydrogen plasma for the analytical determination of oxalic acid is described. The detection limits of 0.75 μmol was obtained from the linear relationship between the peak currents of voltammograms as a function of the oxalic acid concentrations.

1. Introduction

Diamond nanocrystal is a topic of considerable interest in the scientific community, as properties of these systems are expected to retain a large extent of singular characteristics concerning polycrystalline diamond films [1]. Based on the growth chemistries such as argon-rich and hydrogen-poor gas phase, the NCD may be produced with different crystalline structures and grain sizes. Doped NCD films may be grown by adding nitrogen or boron in growth mixture to obtain the n-type or p-type semiconductor materials, respectively, for electronic applications [1]. Boron is the most successful and widely used acceptor in diamond. The success of such doping will be largely dependent on the doping position within the films and the nature of the bonding of the doping atoms to the surrounding of the carbon atoms. Taking into account the BDND electrochemical characteristics, some works have mentioned good results obtained with this electrodes like as fast response, low detection limit, high stability and good response accuracy [2,3].

The use of electrochemical oxidation for the destruction of the organic materials contained in industrial wastewaters has undergone rapid development in recent years in terms of aqueous water treatment. In this sense, the study of electrooxidation of wastes containing carboxylic acids is insipient probably due to their high degree of biodegradability from biological treatment [4]. However, high levels of this specie in the human diet can lead irritation of the digestive system and also can contribute to the formation of kidney stones [5]. Although some works have presented the electrochemistry of the oxalic acid on BDD electrode [4,5], to the best of our knowledge there is no report in the literature of direct oxalic acid oxidation at NCD electrodes.

In this context, the goal of this work is to present the morphological and structural results of NCD and BDND films and described the influence of different surface pre-treatments on these films at the oxalic acid electrooxidation.

2. Experimental details

Depositions were performed using HFCVD technique with the following ones growth parameters: 900 K, 6.7 KPa and 6 h. Gas mixtures were 1/9/90 and 1/19/80 sccm of $CH_4/H_2/Ar$ for NCD and BDND, respectively. Boron was obtained from H_2 forced to pass through a bubbler containing B_2O_3 dissolved in methanol. The doping level corresponds to the acceptor density values around 10^{19} cm^{-3} that were calculated from Mott–Schottky plot measurements (not shown). All films were grown on polished silicon (100) 1×1 cm^2 prepared by ultrasonic hexane bath with 0.25 μm diamond powder during 60 min. The morphology and roughness of the films were evaluated by atomic force microscope (AFM) using a Nanoscope V

* Corresponding author. Tel.: +55 12 3945 6905; fax: +55 12 3945 6717.
E-mail address: adriana@las.inpe.br (A.F. Azevedo).

0925-9635/$ – see front matter © 2010 Elsevier B.V. All rights reserved.
doi:10.1016/j.diamond.2010.01.006

Multimode in air and operated in tapping mode. The quality was analyzed by micro-Raman scattering spectroscopy (Renishaw microscope system 2000) using the 514.5 nm line of an argon ion laser taking the spectra covering the range from 400 to 2000 cm^{-1}.

Electrochemical measurements were carried out using the Autolab PGSTAT 302 equipment with a three-electrode cell. The NCD and BDND films were used as working electrodes and their geometric area in contact with the electrolyte was 0.13 cm^2. The platinum coil and Ag/AgCl electrodes were used as counter and reference electrodes, respectively. Four surface pre-treatments were carried out on electrodes: hydrogen plasma (microwave: 400 W during 20 min); oxygen plasma (pulse discharge: 700 V during 2 min); cathodic polarization (potential: −3.0 V during 30 min) and anodic polarization (current density: 0.5 mA cm^{-2} during 10 s). The cathodic and anodic polarizations were performed in 0.1 mol L^{-1} $HClO_4$ solution. The oxalic acid electrooxidation was studied by Linear Sweep Voltammetry using 0.1 mol L^{-1} $HClO_4$ solution, while the quantitative detection of oxalic acid was analyzed by Square Wave Voltammetry (SWV) using a concentration range from 100 to 2000 μmol L^{-1}. Sessile drop contact angle (CA) measurements were obtained on a Krüss Easy Drop using high-purity deionized water, before and after each surface treatment, at room temperature and atmospheric pressure.

3. Results and discussion

AFM images over a 30 μm × 30 μm area permitted the roughness observation and the grain morphology of NCD and BDND before pre-treatments as shown in Fig. 1a and b, respectively. The surface of both films is flat and not faceted with crystallite sizes around 20–50 nm as observed from AFM images over a 2 × 2 μm (not shown). The film surface roughness of NCD and BDND were very closer around 32 ± 0.2 and 26 ± 0.5 nm, respectively. Although BDND film has been obtained with an argon concentration smaller than that for NCD film, the decrease of its grain size and roughness is associated to the film growth rate decrease with the boron addition as was also observed in other works for BDD films [6,7]. In this way, the average values of films' growth rate were 0.75 and 0.33 ± 0.03 μm for NCD and BDND films, getting films with thicknesses around 4.5 and 2.0 μm, respectively.

There are five and seven features in the Raman spectra of the NCD and BDND films shown in Fig. 2a and b, respectively. The 1332 cm^{-1} diamond peak widens and shifts to lower wavenumber for both films, which is consistent with the Raman result of conductive diamond [2]. However, it is less prominent and obscured by overlapping of the D (1345 cm^{-1}) peak in Raman spectrum of NCD film. The spectra also exhibited two shoulders at 1150 and 1490 cm^{-1} that correspond to transpolyacetylene (TPA) segments at the grain boundaries of NCD surface [8]. For BDND, the peak at 1490 cm^{-1} is stronger than G peak (1560 cm^{-1}) indicating the high proportion of sp^2-bonded carbon in such film. The broad bands around 500 and 1222 cm^{-1} are the subject of some debate [9]. They have been associated with the actual boron incorporation in the lattice, rather than the hole concentration [7].

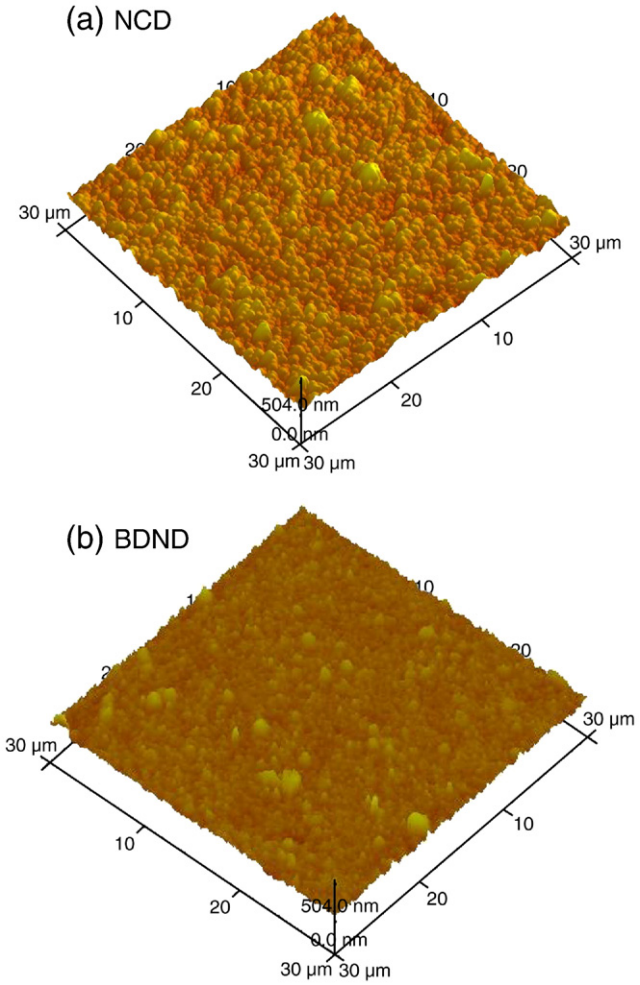

Fig. 1. AFM topographic images of (a) NCD and (b) BDND films, respectively.

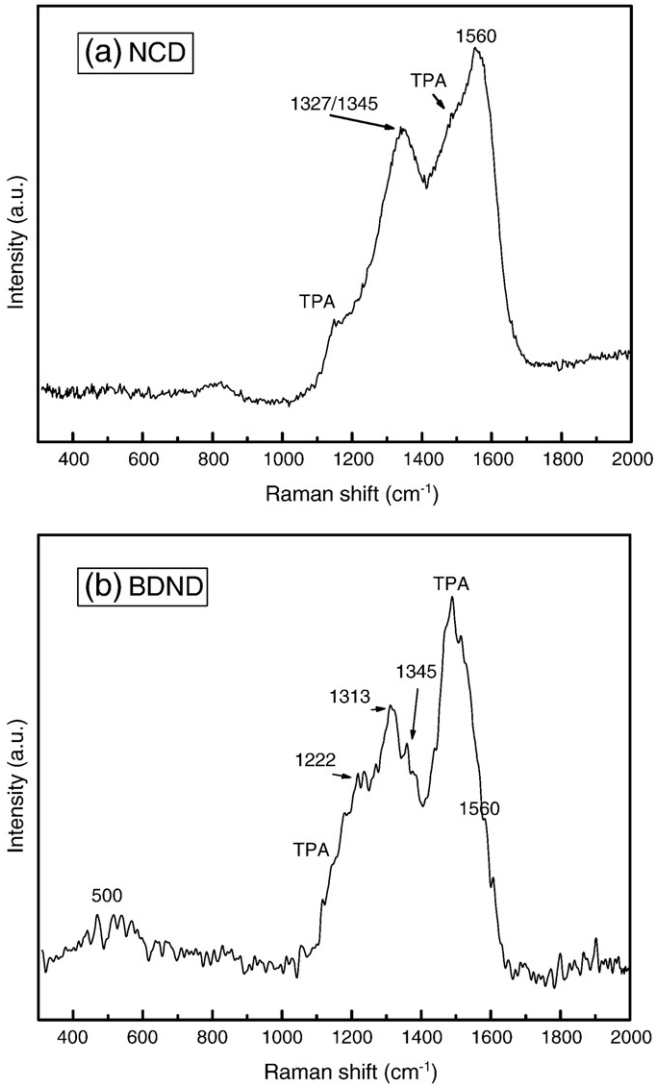

Fig. 2. Raman spectra of (a) NCD and (b) BDND films, respectively.